An experimental investigation on cavitation, noise, and slipstream characteristics of ocean stream turbines

D Wang, M Atlar*, and **R Sampson**
School of Marine Science and Technology, University of Newcastle upon Tyne, Newcastle upon Tyne, UK

The manuscript was received on 23 March 2006 and was accepted after revision for publication on 18 August 2006.

DOI: 10.1243/09576509JPE310

Abstract: The paper presents an experimental investigation on the cavitation, noise, and slipstream characteristics of an ocean tidal stream turbine together with a discussion on the test facilities and methodology used. The experiments were conducted in a cavitation tunnel used to test marine propellers, with the same similarity laws as are used for a marine propeller. The cavitation patterns were observed at conditions corresponding to pre-stall, stall, and post-stall stream speeds as well as for two different depths of submergence of the turbine shaft to simulate the static presence of waves. The noise levels of the turbine were measured at the same conditions as the cavitation tests. The experimental results show that the turbine can experience strong unstable sheet and cloud cavitations as well as strong tip vortex cavitation at a shallow depth of shaft submergence which can be imposed by a wave trough taking place over the turbine. It is also shown that the measured noise level of the turbine is further increased due to the presence of cavitation. Finally, the slipstream wash was measured in terms of field velocities in the wake and surrounding of the turbine, and results show the slipstream wash may have an impact on the seabed if a turbine is positioned too close to it.

Keywords: renewable energy, ocean stream/marine turbine, cavitation, noise, slipstream wash, environmental impact

1 INTRODUCTION

Owing to increasing demand in clean energy and rising fossil fuel prices, more and more investment and research are focused on the renewable energy resources. These include electricity extracted from wind resources by means of wind turbines, and more recently, from tidal and other current resources in oceans through water turbines. Offshore renewable resources such as offshore wind, tidal stream/current, and waves are the most abundant source of renewable energy on the earth. It is more realistically estimated that extractable tidal stream energy are about 18 TWh/yr within UK continental shelf and channel island territorial sea [**1**]. Much effect had been made to extract tidal energy through various demonstration projects, including fixed prototype installation [**2**, **3**] and some novel floating types [**4**].

The energy extracted from these resources is clean energy because of no emissions of CO_2 in the production of energy; however, this does not mean that it is free from impact on the environment. Although the impact of the wind turbines on the environment has been widely investigated [**5**–**9**], to the authors' knowledge, there is hardly any investigation reported in the open literature to explore potential sources for environmental impact associated with tidal stream turbines.

In harnessing energy from the ocean a tidal stream turbine operates on the similar principle as the wind turbine, except that tidal steam turbines are prone to cavitation phenomena and free surface effects and hence it will produce and radiate undesirable noise due to shedding vortices from its blades and supporting tower. Unlike wind turbine, a tidal stream turbine will not have an undesirable, direct 'visual' impact nor 'noise' effect on human beings since the turbine

**Corresponding author: School of Marine Science and Technology, University of Newcastle Upon Tyne, Newcastle Upon Tyne, NE1 7RU, UK. email: mehmet.atlar@ncl.ac.uk*

will be deeply submerged in the sea. However, it will have a potential impact on the environment, in particular sea life when one considers the concept of 'energy farms', which include arrays of these units in a concentrated area, and increased noise radiation and scouring effect at sea bed.

An important difference between wind and tidal stream turbines is the potential cavitation phenomena that may occur on the blades of the tidal turbine which can increase the risk of environmental impact as well as causing erosion on the blades.

The cavitation phenomenon was first observed and reported scientifically on marine propeller over a hundred years ago [**10**, **11**]. Although the onset of cavitation on a marine propeller blade is rather complex phenomenon mainly involving the effect of operating condition, blade geometry, and water quality, in simple terms one can assume that cavitation will develop at any point on the blade where the pressure level is reduced to the level of saturated vapour pressure of the ambient water. When such an equilibrium condition is reached, different types of cavitation may develop (e.g. tip vortex, sheet, bubble, cloud etc.) depending on the above-mentioned effects. As a stream turbine operates on the same principle as a marine propeller, it can be subjected to some of these types of cavitation phenomena.

Depending on the type of the cavitation developed, some undesirable effects can be allied with it, including erosion of the blade, due to imploding cavities near to the blade surfaces and associated noise as well as shaft vibration and performance degradation depending on the extent, volume, and fluctuating nature of the developed cavitation. The radiated noise level of a stream turbine will be increased considerably due to the presence of cavitation which will cause further environmental concern on the surrounding sea life. The issue of designing a stream turbine incorporating with cavitation, in particular, based on the wind turbine blade technology, is being currently overlooked. There are recent studies reported in the open literature, e.g. Batten *et al.* [**12**] and Molland *et al.* [**13**], where attempts were made to minimize or avoid cavitation in the design of current turbines based on cavitation free bucket analysis of two-dimensional sections, a method used in marine propeller design. In these joint studies, various two-dimensional NACA sections were used and their cavitation characteristics were validated with cavitation tunnel tests based on these two-dimensional, stationary foils. No experimental investigation was reported on the cavitation performance of the whole turbine model in the issue of environmental impact.

Another source of potential environmental impact, that can be associated with a tidal stream turbine, is the perturbed velocity field and associated wash effect induced by the vortices in the slipstream of the turbine. Although the slipstream wash of a marine propeller has been investigated by many researchers, including the present authors [**14**–**16**], no similar investigations have been reported on stream turbines in the open literature to the authors' knowledge.

The present paper, therefore, aims to contribute to the above-mentioned knowledge gaps through an experimental investigation on the cavitation, noise, and slipstream wash characteristics of a tidal stream turbine by adopting the testing and extrapolation procedures used for marine propellers. The details of the testing facility is described next and this followed by the description of the cavitation observations, noise, and slipstream wash measurements with a 400 mm tidal stream turbine model, including the discussion of the results and conclusions from the investigation.

2 TESTING FACILITY AND METHODOLOGY

2.1 Test facilities and model

The experiments were conducted in the emerson cavitation tunnel (ECT) at the Newcastle upon Tyne University. The tunnel is a medium size propeller cavitation tunnel with a measuring section of 1219 mm × 806 mm (width × height). The speed of the tunnel water varies between 0.5 and 8 m/s, whereas the tunnel pressure can be varied to give a tunnel speed based cavitation number of 0.5–23. Full details of the ECT can be found in reference [**17**].

The full-scale turbine has a 20 m diameter with three blades and was designed based on a stall regulation to operate in a design tidal stream speed of 3.5 m/s and shaft speed of 12 r/min. The airfoil type S814 section [**18**] was used in the design of the blade sections. A 1/50th scaled model of the turbine, which has a 400 mm diameter, was made from brass alloy material with built-in blades for the experiments, and the main particulars of the model are presented in Table 1.

The turbine was driven by the propeller drive system of the ECT, and the torque and thrust of the turbine were measured by using the tunnel's main dynamometer (K&R Type H33) in order to set and control the operating condition of the turbine accurately. Using the same setup, the sound pressure levels of the turbine were measured by using Bruel & Kjaer Type 8103 miniature hydrophone and associated data acquisition system, whereas the flowfield around the turbine was measured by means of a two-dimensional Dantec laser doppler anemometry (LDA) system. Further details of these systems and the tests are given in the following.

Table 1 Main particulars of the tidal stream turbine models

r/R	0.2	0.3	0.4	0.5	0.6	0.7	0.8	0.9	1
Chord length (mm)	64.35	60.06	55.76	51.47	47.18	42.88	38.59	34.29	30
Twist angle (°)	27	15	7.5	4	2	0.5	−0.4	−1.3	−2

2.2 Test methodology

It is well known that in order to properly simulate the real operating condition in the experimental environment, certain similarity laws have to be observed. Although a marine propeller and a tidal stream turbine have different missions, they operate based on the same hydrodynamic principles in experiencing the hydrodynamic loadings developed on their blades, including the effects of cavitation and free surface. Thus, the well-established similarity laws for the propeller flow are adopted for a stream turbine in the present experimental investigations, which include two basic similarity laws, i.e. geometry similarity and flow or hydrodynamic similarity.

2.2.1 Geometry similarity

Geometry similarity will require the tested model should have similar geometry as that in the fullscale. This similarity can be easily achieved by scaling down the full-scale geometry using a fraction, or so-called scale factor. The scale factor should be chosen as larger as possible according to test facilities in order to reduce Reynolds number related scale effect on test results, and it was chosen as 1/50 based on test facilities of ECT.

2.2.2 Flow or hydrodynamic similarity

The hydrodynamic similarity of a marine propeller is presented by following non-dimensional coefficients.

Advance ratio

$$J = \frac{V_c}{nD} \tag{1}$$

Cavitation number

$$\sigma = \frac{p - p_v}{0.5\rho V_R^2} \tag{2}$$

Reynolds number

$$R_e = \frac{C_{0.7R} V_R}{\nu} = \frac{C_{0.7R}\sqrt{V_c^2 + (0.7D\pi n)^2}}{\nu} \tag{3}$$

Froude number

$$F_n = \frac{V_c}{\sqrt{gD}} \tag{4}$$

Gas content ratio

$$\frac{p}{p_a} = \frac{\alpha}{\alpha_s} \tag{5}$$

The conduct of the cavitation tests in a cavitation tunnel with no free surface would only require the constant 'advance ratio' and 'cavitation number' for the model and full-scale propeller while the compliance with the constant 'Reynolds' and 'Froude' numbers will be violated due to physical limitations of a testing facility and absence of the free surface, respectively. In the case of a turbine, the advance ratio of a propeller can be replaced with a more representative 'tip speed ratio' (TSR) of the turbine flow, whereas the cavitation number at a interest point on the blade of a turbine (e.g. 0.7 R) can be defined, basically, similar to the propeller cavitation number. Thus the TSR, λ, can be described as

$$\lambda = \frac{\pi D n}{V_c} \tag{6}$$

Like in most of other hydrodynamic tests, Reynolds number, R_e, which is defined in equation (3), cannot be fully simulated, and it should be set as high as possible in order to reduce the associated scale effect. From the experience with marine propeller model tests, when R_e is higher than 10^6, the associated scale effect can be assumed negligible. By considering the physical limitations of the ECT facility, R_e was set at about $0.2–0.3 \times 10^6$ in the present tests.

As stated earlier, the water quality is an important factor in cavitation phenomenon, whose effect can be represented, in the simplistic terms, by the dissolved gas or oxygen content of the tunnel solution, although its distribution is equally important. The level of this content should be maintained at a required level in order to minimize the resulting scale effects. In the present tests, the dissolved oxygen content was measured and controlled by means of YSI model 95 handheld dissolved oxygen and temperature system.

3 CAVITATION OBSERVATIONS

3.1 Operating conditions

Cavitation observations were carried out in three different conditions corresponding to pre-stall, stall (designed), and post-stall stream speeds, to cover a range of stream speeds that might induce cavitation.

The upper and lower limits of this range were specified in such a way that two thirds of the maximum power, which is represented by 67 per cent of Cp_{max}, as shown in Fig. 1, is extractable and from which the two-limit tip speed ratios and, hence, the corresponding pre- and post-stream speeds are specified.

Tests were conducted corresponding to two different depths of turbine shaft submergence, the designed (20 m) and shallow (11 m) shaft immersion. The latter condition was used to simulate the effect of waves on cavitation in terms of the static water head representing the trough of a wave while dynamic effect of waves was ignored due to limit of test facilities. Of course this is too simplistic way of simulating the wave effect since the dynamic action of the wave particles and other realities would be ignored. However, full simulation of the entire wave effects would require more sophisticated testing facilities (e.g. vacuum tank with wave maker) and associated setup which was beyond the scope of this investigation. Table 2 presents a summary of operating conditions and other details of the turbine and flow in the full-scale and model-scale.

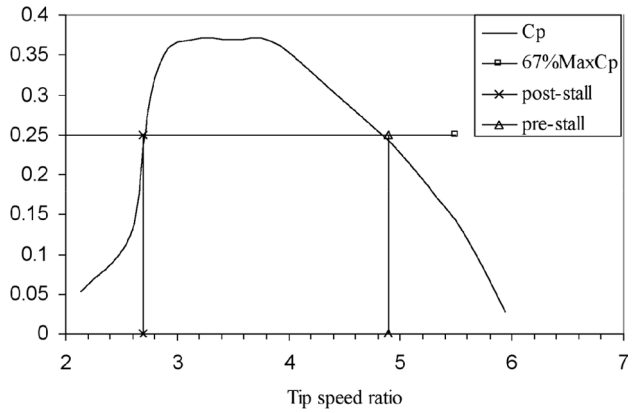

Fig. 1 Definition of pre- and post-stall stream speeds

In Table 2, the static head (Hs) denotes the shaft immersion in full scale, whereas in model scale the value of Hs is met by the amount of vacuum applied to the tunnel to keep the cavitation number as same as that in full-scale. The model scale Hs value was measured and controlled by a 'U' type mercury manometer in ECT; the dissolved oxygen content level (α/α_s) was kept constant throughout the tests at 42 per cent.

3.2 Cavitation observations at designed shaft immersion (20 m)

Figures 2 to 4 show the observed cavitation patterns corresponding to the designed, pre-, and post-stall stream speeds at the designed shaft immersion and constant rate of rotation of the turbine shaft, respectively. As shown in Fig. 2, only mild tip vortices were observed at the designed stream speed which will also result in an increase in the noise level as it will be discussed later on.

Cavitation pattern at the pre-stall stream speed manifested itself in a much finer and intermittent type of tip vortex as shown in Fig. 3.

As shown in Fig. 4, different to the cavitation patterns observed in the previous two conditions, the cavitation type observed at the post-stall stream speed was only a very light sheet cavitation developed at the leading edge of the suction side of the blades extending from 0.55 to 0.7 R and there was no tip vortex observed.

3.3 Cavitation observed at shallow shaft immersion (11 m)

As stated earlier in order to explore the effect of waves, particularly the effect of a wave trough, the turbine was tested at much shallower shaft immersion (11 m as opposed to 20 m designed immersion in full scale). Similar to those at the designed submergence, cavitation observations were made at the designed, pre-, and post-stall stream speeds under the same

Table 2 Operating conditions and other details

	Full scale						Model scale					
	Design	Pre-stall	Post-stall	Design	Pre-stall	Post-stall	Design	Pre-stall	Post-stall	Design	Pre-stall	Post-stall
V_c (m/s)	3.5	2.57	4.67	3.5	2.57	4.67	2	1.47	2.67	2	1.47	2.66
n (r/min)	12	12	12	12	12	12	342.9	342.9	342.9	342.9	342.9	342.9
D (m)	20	20	20	20	20	20	0.4	0.4	0.4	0.4	0.4	0.4
λ	3.59	4.89	2.69	3.59	4.89	2.69	3.59	4.89	2.69	3.59	4.89	2.69
Hs (m)	20	20	20	11	11	11	−0.2	−0.2	−0.2	−0.435	−0.435	−0.435
σ	3.7890	3.988	3.499	2.232	2.349	2.061	3.7890	3.988	3.499	2.232	2.349	2.061
α/αs							42%	42%	42%	42%	42%	42%

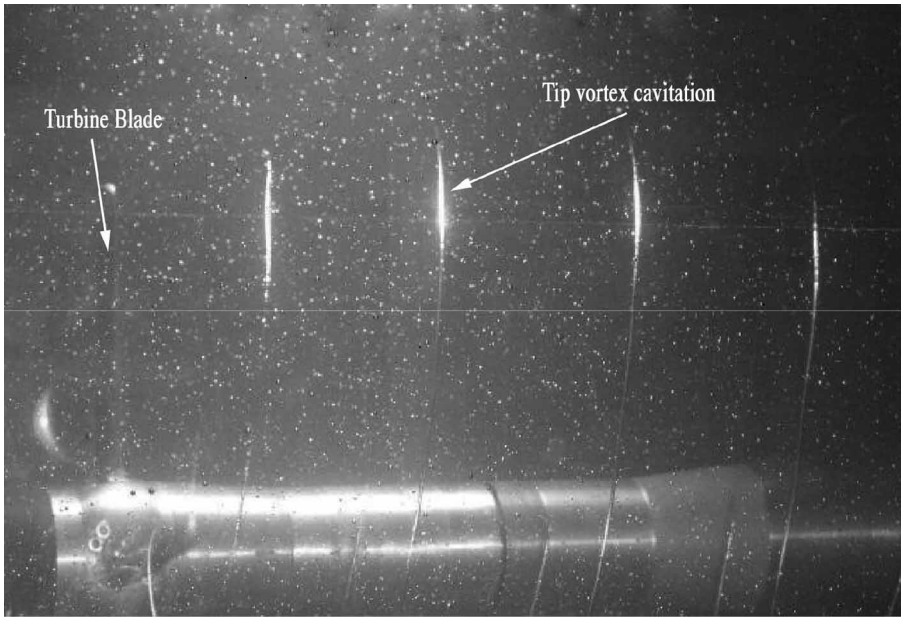

Fig. 2 Cavitation observed at designed shaft immersion and stream speed ($V_c = 3.5$ m/s, $n = 12$ r/min, Hs = 20 m, $D = 20$ m, TSR = 3.69, $\sigma = 3.789$)

oxygen content, and observed cavitation patterns are shown in Figs 5, 6, and 7, respectively.

As shown in Fig. 5, the designed stream speed displays considerably thick but stable sheet cavitation on the blades extending over the region from 0.6 to 0.9 R and from the leading edge to the maximum of 20 per cent chord length. However, the tail end of the sheet cavitation displays some instability and bursts to form an unstable and erosive cloud cavitation. In this condition, relatively thick and strong tip vortices emanating from the blades were also observed.

However, at the pre-stall stream speed, as shown in Fig. 6, only stable thin tip vortices were observed.

Finally, Fig. 7 shows the cavitation observed at the post-stall stream speed. In this condition, more extended and thicker sheet cavitation were observed in the region from 0.5 to 0.9 R and from leading edge to the maximum of 30 per cent chord length. Similar to the designed condition, the tail end of the sheet

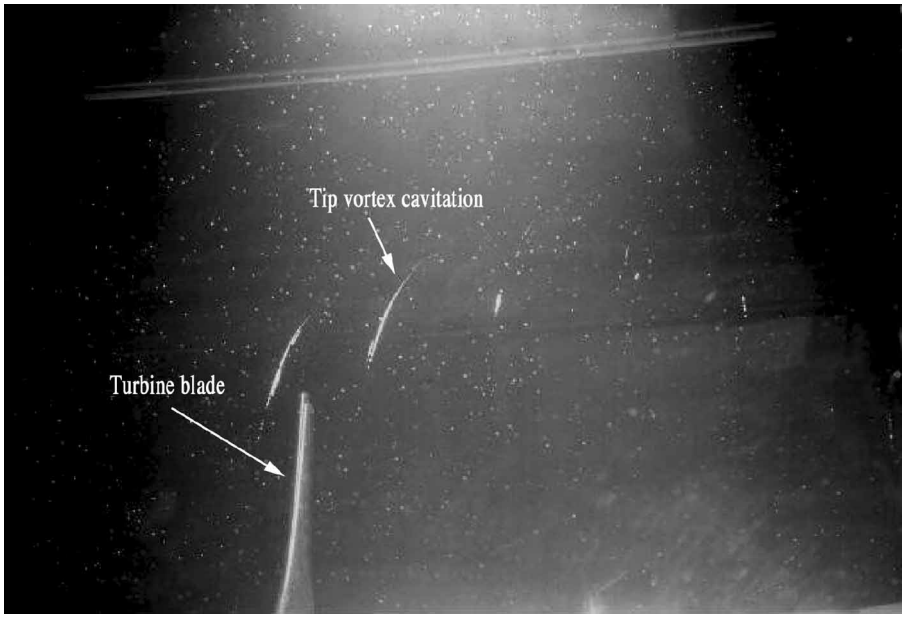

Fig. 3 Cavitation observed at designed shaft immersion and pre-stall stream speed ($V_c = 2.57$ m/s, $n = 12$ r/min, Hs = 20 m, $D = 20$ m, TSR = 3.69, $\sigma = 3.933$)

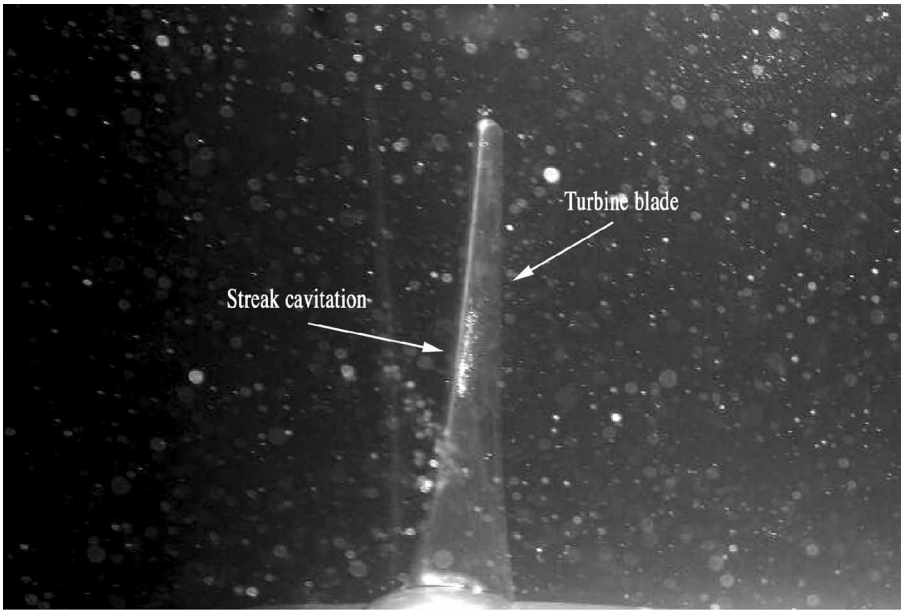

Fig. 4 Cavitation observed at designed shaft immersion and post-stall stream speed ($V_c = 4.67$ m/s, $n = 12$ r/min, Hs = 20 m, $D = 20$ m, TSR = 3.69, $\sigma = 3.499$)

cavitation became unstable and burst to form erosive cloud cavitation in combination with much stronger tip vortices shedding from the blades making the situation worst.

4 NOISE MEASUREMENTS

The noise level measurements of the turbine were conducted simultaneously with the cavitation observations and, hence, at the same test conditions presented in Table 2.

4.1 Test set-up and procedures

The common procedure of noise measurements in the emerson cavitation tunnel is to use Bruel & Kjaer Type 8103 Miniature Hydrophone. This device was situated in a water-filled, thick-walled, steel cylinder placed on Plexiglas window outside the

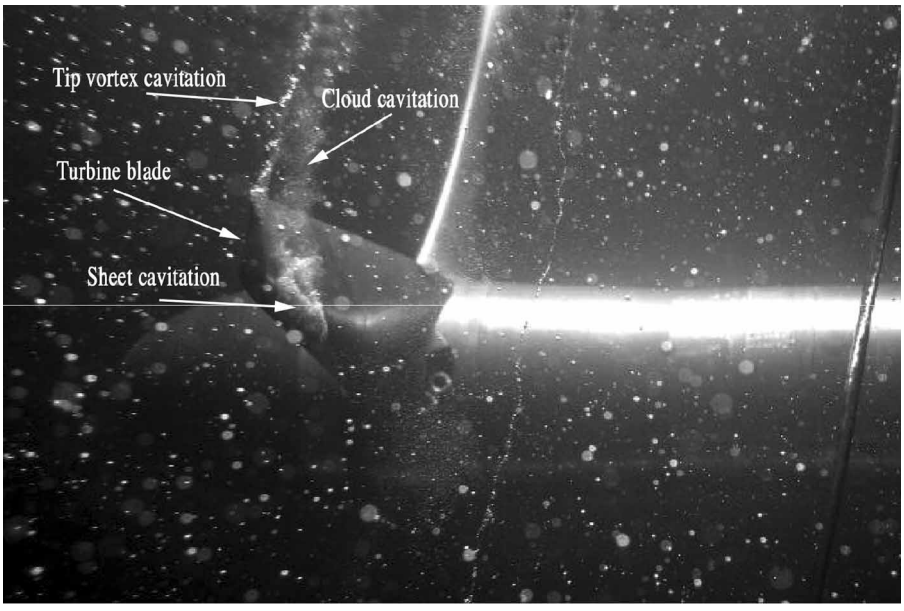

Fig. 5 Cavitation observed at shallow shaft immersion and designed stream speed ($V_c = 3.5$ m/s, $n = 12$ r/min, Hs = 11 m, $D = 20$ m, TSR = 3.69, $\sigma = 2.232$)

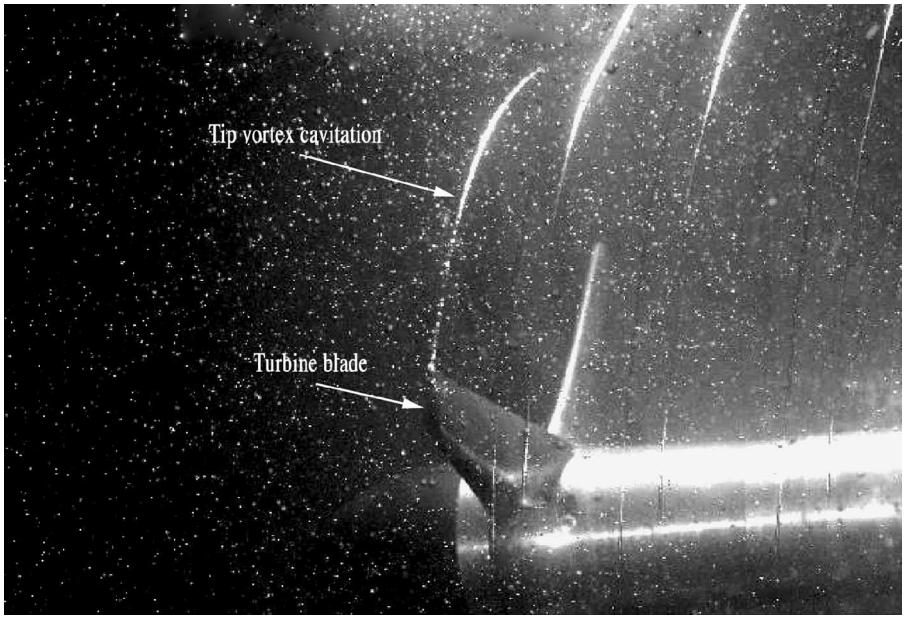

Fig. 6 Cavitation observed at shallow shaft immersion and pre-stall stream speed ($V_c = 2.57$ m/s, $n = 12$ r/min, Hs = 11 m, $D = 20$ m, TSR = 4.89, $\sigma = 2.349$)

top lid of the tunnel and at a vertical distance of 440 mm from the shaft centre-line and 50 mm forward of the rotation plane of the turbine. Bruel & Kjaer PULSE^{TM} Noise and Vibration Analysis – Type 7700 software was used to acquire and analyse the sound pressure data.

The total noise levels of the turbine at one-third Octave band were first recorded at centre frequencies ranging from 20 Hz to 25 kHz, which included both the net turbine noise and the noise generated by the proximity (background noise). Consequently, in order to calculate the noise generated exclusively by the turbine, i.e. the net turbine noise, the background noise had to be measured separately and to be subtracted logarithmically from the total measured noise. In the measurements of the background noise, an idle mass, which had the same mass as model turbine, replaced the model turbine

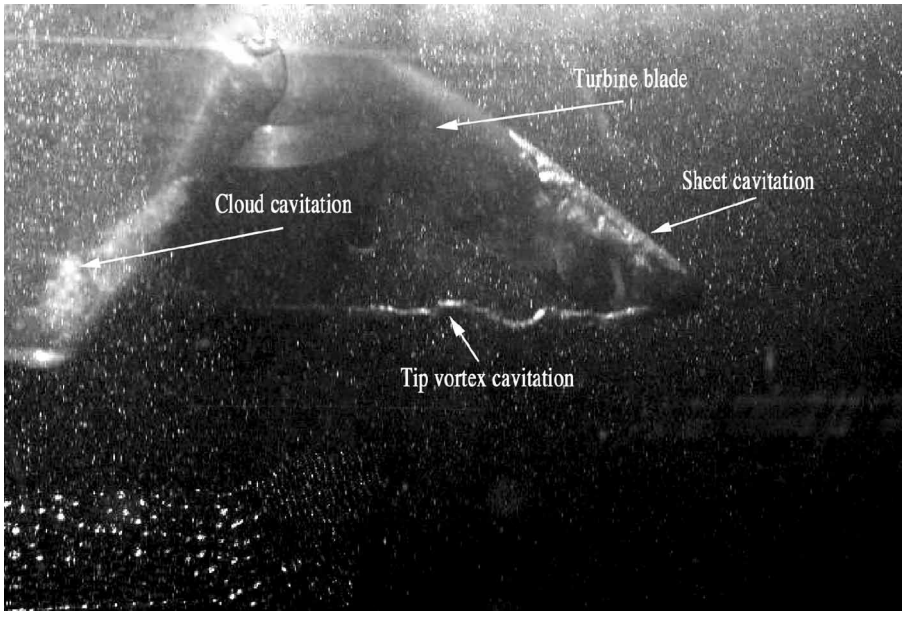

Fig. 7 Cavitation observed at shallow shaft immersion and post-stall stream speed ($V_c = 2.57$ m/s, $n = 12$ r/min, Hs = 11 m, $D = 20$ m, TSR = 4.89, $\sigma = 2.349$)

and the tunnel was kept working at the same operating condition and having the same water quality as for the total noise measurements carried out previously.

4.2 Results analysis

A common practice in the analysis and presentation of the noise levels for a ship propeller are to reduce the measured values of sound pressure levels (SPL) in each one-third Octave band to an equivalent 1 Hz bandwidth by means of the correction formula recommended by the cavitation committee of the 15th International Towing Tank Conference (ITTC) as follows [**19**]

$$\mathrm{SPL}_1 = \mathrm{SPL}_\mathrm{m} - 10\log\Delta f \tag{7}$$

The ITTC also required that the sound pressure levels be corrected to a standard measuring distance of 1 m using the following relationship

$$\mathrm{SPL} = \mathrm{SPL}_1 + 20\log(r) \tag{8}$$

Having converted the measured SPL_m for the total and the background noise sources to the equivalent 1 Hz at 1 m SPL_1 using equations (7) and (8), the level of net sound pressure (SPL_N) of the model propeller at each centre frequency was calculated using the following logarithmic subtraction formula given by Ross [**20**],

$$\mathrm{SPL}_\mathrm{N} = 10\log\left[10^{(\mathrm{SPL}_\mathrm{T}/10)} - 10^{(\mathrm{SPL}_\mathrm{B}/10)}\right] \tag{9}$$

The noise level of the model propeller was extrapolated to the full-scale noise level using scaling laws recommended by the Cavitation Committee of 18th ITTC [**21**]

$$\Delta L_{(p)} = 20\log\left[\left(\frac{D_\mathrm{P}}{D_\mathrm{M}}\right)^z\left(\frac{r_\mathrm{M}}{r_\mathrm{P}}\right)^x\left(\frac{\sigma_\mathrm{P}}{\sigma_\mathrm{M}}\right)^{y/2}\left(\frac{n_\mathrm{P}D_\mathrm{P}}{n_\mathrm{M}D_\mathrm{M}}\right)^y\left(\frac{\rho_\mathrm{P}}{\rho_\mathrm{M}}\right)^{y/2}\right] \tag{10}$$

$$f_\mathrm{P} = f_\mathrm{M}\frac{n_\mathrm{P}}{n_\mathrm{M}} \tag{11}$$

where subscripts P and M refer to ship and model, respectively; z and y are taking as 1 and 2, respectively.

In the presence of no specific code of practice for water turbines, the above-described analysis method for ship propellers was adopted to predict the net sound pressure levels of the full-scale turbine for all the test conditions and results are shown in Figs 8 and 9. In the absence of a specific criterion to control noise radiated from such devices, the minimum noise specification recommended by the International Council for the Exploration of the Sea (ICES) for fisheries research vessel was also presented in these figures for reference only [**22**]. This specification is to meet the need for noise reduction in research vessels undertaking fishery resource surveys and makes practical recommendation for limiting underwater radiated noise, to assist those drawing up specifications for new vessels. On this basis, it does not provide any regulatory value apart from an interesting comparison.

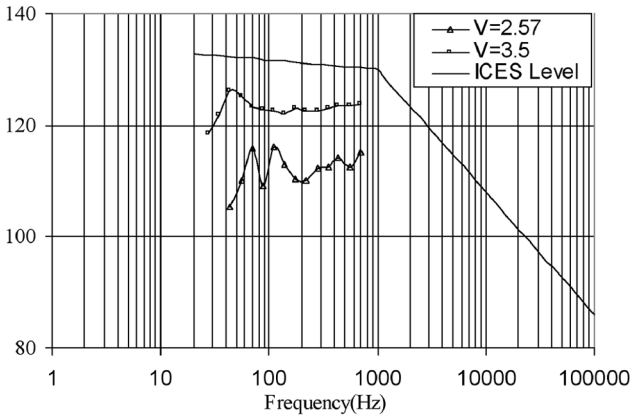

Fig. 8 Net noise levels at designed shaft depth in the full scale

Figure 8 presents a comparison of the net noise levels of the turbine at the pre-stall and designed stream speeds for the design shaft immersion (20 m). The condition for the post-stall speed was excluded since the background noise level in this case was higher than the total noise level which unfortunately does not reflect any meaningful result. As shown in Fig. 8, within the measured region, the predicted net noise level at the designed speed is about 10–15 per cent higher than the pre-stall stream speed condition reflecting the contribution from

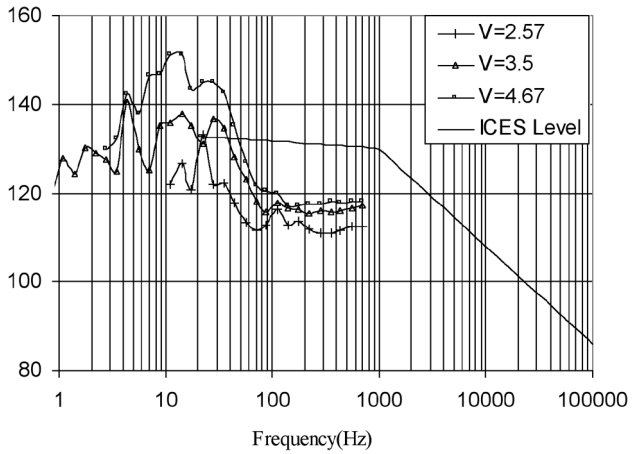

Fig. 9 Net noise levels at shallow shaft depth in the full scale

relatively more prominent tip vortices for the former condition. It is also interesting that both conditions display lower noise levels in comparison to the ICES minimum noise specification criteria.

Figure 9 presents a comparison of the net noise level of the turbine at the pre-stall, designed, and post-stall stream speeds at the shallow shaft immersion (11 m). Except the pre-stall condition at lower frequency range (i.e. $<$10 Hz), majority of the predicted net noise for all conditions appears to be free from the background noise contamination. The net SPL can be as high as 150 dB at the post-stall condition and there is a hierarchy in the increasing noise levels regarding to the increasing magnitude of the stream speed and hence severity of the cavitation patterns observed earlier. It is also interesting to note that the SPL for the design and post-stall speeds can be higher than the ICES specification level over some part of the low-frequency range.

In spite of the uncertainty associated with the background noise over a certain frequency range, the comparison of the net SPLs in Figs 8 and 9 indicates that the noise levels increase with the increase of intensities of the tip and unstable cloud cavitations, particularly in the medium range of centre frequencies (5–30 Hz) investigated.

5 SLIPSTREAM WASH MEASUREMENT

On the basis of the assumption that the potential impact of the tidal stream turbine on environment (e.g. scouring of the sea bed, increased noise) will manifest itself through the perturbed velocities in the turbine's slipstream, the velocity field in this wake region was measured by means of a LDA in the ECT.

5.1 Test setup and procedures

The LDA used was a two-dimensional Dantec LDA whose optic was controlled by a computer driven three-dimensional traversing mechanism. A polar coordinate system was used for setting the measurement mesh which was selected in the bottom left quadrant along the turbine shaft, due to limitation on the access to the full-slipstream. On each mesh quadrant, nine angles (10 points), at 10° intervals, were set in the circumferential direction. In the radial direction, 18–24 radii were specified with the maximum radius being 280 mm. A Cartesian coordinate system was selected with its origin located at the shaft axis and 30 mm in front of the turbine disc plane. The measured slipstream length was approximately one full diameter (410 mm). This was selected such that a distance equivalent to 1 R of the turbine (200 mm) was behind the disc and 1.05 R (210 mm) was in front of the disc along the x-direction; eight quadrant meshes were used to cover this measurement length, as shown in Fig. 10.

The velocity field behind a propeller or turbine is unsteady and it is difficult to measure this flowfield using the LDA technology since it is time dependent and data acquisition will require an enormous amount of data samples and associated time. Fortunately, although the turbine wake is unsteady, it is periodic and can be measured using encoder technology. The periodic nature of the flow motion can imply to acquire as many samples as required at a space point, provided that the samples are acquired using an encoder to trigger the acquisition. The function of the encoder is to trigger all the measurements starting at the same time in a cycle and this will guarantee each sample is acquired at the same time in a period. The encoder is triggered by a transistor-transistor-logic pulse, equating to one pulse per turbine revolution.

5.2 Results analysis

The velocity field measurements were carried out at the turbine designed operating condition which

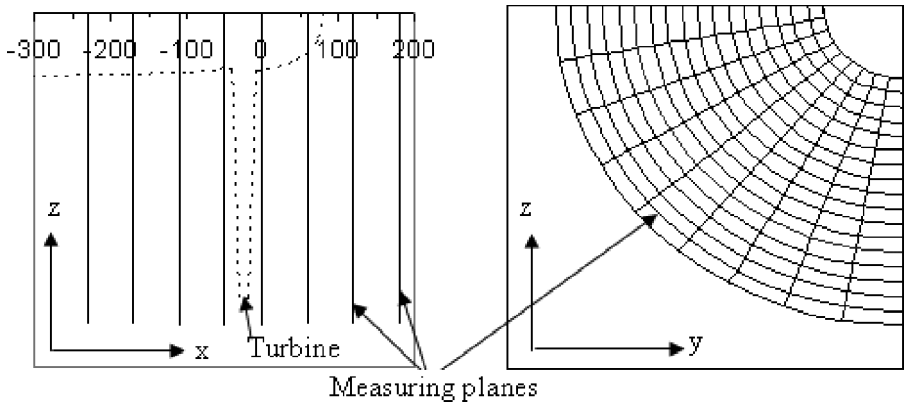

Fig. 10 Arrangement of measuring meshes

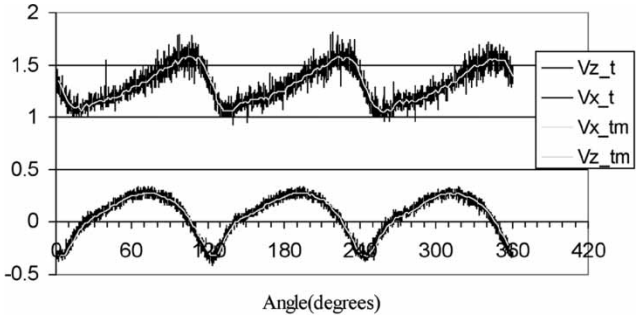

Fig. 11 Measured total velocities in time domain

corresponds to a 2 m/s of stream speed and 342.9 r/min of shaft rotation rate. At each measuring point, about 3000–4000 velocity samples were collected for each of the two velocity components (V_x, V_z) within one turbine revolution. From these samples, 72 velocity data per velocity component are averaged at 5° intervals within one revolution as shown in Fig. 11 where V_{x_t} and V_{z_t} are the measured velocity samples in time domain and V_{x_tm} and V_{z_tm} are the mean velocities averaged at each 5° interval.

At each measured point, 72 velocity data for each velocity component were further averaged in time domain based on the following integration to obtain the mean velocity at one measuring point

$$V_{x\_p\mathrm{m}} = \frac{1}{2\pi}\int_0^{2\pi} V_{x\_t\mathrm{m}}\,\mathrm{d}\theta \tag{12}$$

$$V_{z\_p\mathrm{m}} = \frac{1}{2\pi}\int_0^{2\pi} V_{z\_t\mathrm{m}}\,\mathrm{d}\theta \tag{13}$$

At each radius of the measured quadrant, $V_{x\_p\mathrm{m}}$ and $V_{z\_p\mathrm{m}}$ were averaged to obtain the mean velocity at a radius as follows

$$V_{x\_r\mathrm{m}} = \frac{2}{\pi}\int_0^{\pi/2} V_{x\_p\mathrm{m}}\,\mathrm{d}\theta \tag{14}$$

$$V_{z\_r\mathrm{m}} = \frac{2}{\pi}\int_0^{\pi/2} V_{z\_p\mathrm{m}}\,\mathrm{d}\theta \tag{15}$$

On each measured quadrant, $V_{x\_r\mathrm{m}}$ and $V_{z\_r\mathrm{m}}$ were averaged to obtain the mean velocity on each quadrant as follows

$$V_{x\_\mathrm{m}} = \frac{1}{R-r_\mathrm{h}}\int_{r_\mathrm{h}}^{R} V_{x\_r\mathrm{m}}\,\mathrm{d}r \tag{16}$$

$$V_{z\_\mathrm{m}} = \frac{1}{R-r_\mathrm{h}}\int_{r_\mathrm{h}}^{R} V_{z\_r\mathrm{m}}\,\mathrm{d}r \tag{17}$$

The mean axial velocities thus calculated at each radius on each quadrant are shown in Fig. 12.

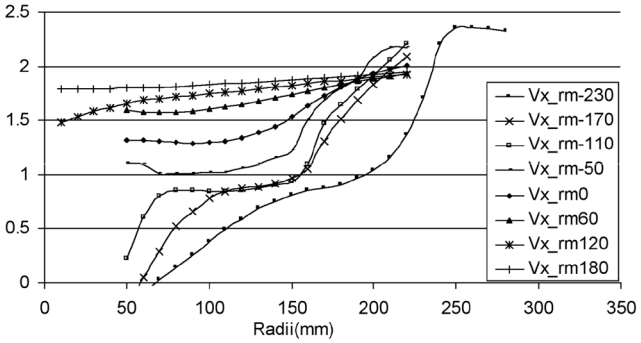

Fig. 12 Measured mean axial velocity $V_{x\_r\mathrm{m}}$ (averaged at a radius)

Useful insight to the distributions of the mean longitudinal velocity component (V_x) along the shaft axis both before and after the turbine disc and along the radii can be gained. The striking feature of this flowfield is the increasing magnitudes of the velocity component V_x at the outer radii towards/beyond the tip in the downstream. The magnitude of the perturbed velocity component V_x can be 17 per cent higher than the free stream speed at a fractional radius of $r/R = 1.4$ from the shaft axis in the measurement plane, $x = -230$ mm (i.e. at a downstream distance of 1.0 R). Thus, the total velocity (resultant velocity of V_x, V_y and V_z) will be surely higher than 17 per cent and the expected slipstream wash might have impact on the seabed (e.g. adverse scouring effect), if the turbine is to be installed close to the seabed.

The variation of the mean vertical component (V_z) of the velocity field along the shaft and radii, as shown in Fig. 13, displays rather complex distribution without any clear trend, although the magnitudes of the velocities increase towards and after the turbine in the near vicinity.

Although the magnitudes of V_z in overall are much smaller than the magnitudes of the axial component

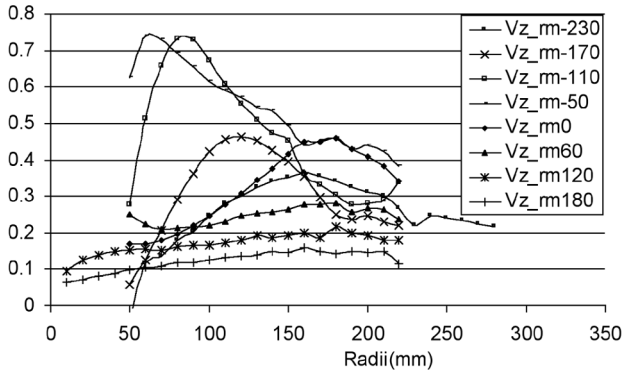

Fig. 13 Measured mean vertical velocity $V_{z\_r\mathrm{m}}$ (averaged at a radius)

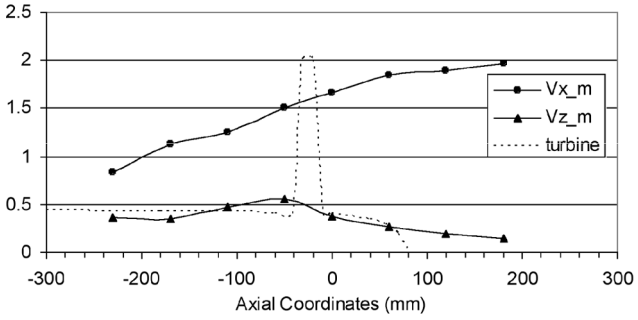

Fig. 14 Measured mean axial and vertical velocities (averaged at a quadrant)

(V_x), being about one third of the latter at the maximum, they will contribute and hence increase the magnitude of the total velocities.

Variations of the mean velocity on each measured quadrant are shown in Fig. 14, which presents mean velocity variations in the process of flow passing through the turbine. From Fig. 14, it seems that there will be no concern of the environmental impact from the turbine slipstream wash within its wake as dominant component V_x of wash velocity is much less than stream speed. It also reveals some interesting velocity variations, although not relevant within the wash context: firstly, the value of the mean stream velocity is reduced as the flow approaches to the rotor disc due to blocking effect of the turbine; and secondly, it is noticed that that the rotor induces a swirling action to the flow, and it seems that the maximum value of the swirl is reached at the disc and then this action decays in the wake due to viscous effect.

6 CONCLUSIONS

From the present investigation, the following conclusions can be reached.

1. Cavitation tunnels and testing procedures used for marine propellers can be used and adopted for testing marine turbines to investigate their performance in the likely presence of cavitation.
2. Cavitation can be an important design and environmental concern for a tidal stream ocean turbine if the turbine blades are not properly designed and the turbine is not properly installed.
3. Extreme waves can have significant influence on cavitation performance as a result of the statically reduced immersion of the turbine shaft and the dynamically increased flow velocity at the turbine blade due to effect of the free surface, though the later was not tested in present paper. The immersion of 1.5–2.0 diameter of turbine should be required to avoid such effect without deteriorating performance of power extraction.
4. Cavitation also increases the level of noise radiated from the turbine and hence can be a further source of concern for the marine environment, in particular in a 'farm' configuration.
5. Slipstream wash velocity of a tidal stream turbine can be significantly higher than the free stream velocity which may have an adverse effect on the seabed as well as contributing to the radiated noise levels. The turbine shaft should be kept clear from the seabed at least for one turbine diameter distance to avoid such impact.
6. In occurrence of severe cavitation, a stream turbine may have significant impact on environment in terms of noise. If a stream turbine is too close seabed (shaft height from seabed is less than one diameter of the turbine), the turbine may have impact on environment by causing sediment movement on seabed or disturbing marine life near seabed.

ACKNOWLEDGEMENT

The present investigation was based on the part of the results of a joint research project entitled 'An investigation of tidal stream rotor performance', EPSRC Grant Ref no: GR/R50851/01, and was conducted during 2002–2005. This project was sponsored by the EPSRC's 'Renewable & New Energy Technologies' Programme- RNET4/308 and hence the financial support received by the EPSRC is gratefully acknowledged.

REFERENCES

1 **Black & Veatch Consulting Ltd.** *Phase II UK tidal stream energy resource assessment*. Phase II tidal stream resource report–rev2.doc, Issue 3, July 2005, available from www.thecarbontrust.co.uk/ctmarine3/res/PhaseIITidalStreamResourceReport.pdf.

2 **Fraenkel, P. L.** Power from marine turbines. *Proc. Instn Mech. Engrs, Part A: J. Power and Energy*, 2002, **216**(A1), 1–14.

3 **Fraenkel, P. L.** Marine Current Turbines^{TM} Ltd's tidal turbines developments: the development of an entirely new energy conversion system. Part D Conference Proceeding of World Maritime Technology Conference (WMTC), 4th International Marine Renewable Energy, MAREC, London, 6–10 March 2006, pp. 79–88, IMarEST.

4 **Manchester, R.** The TidEl floating free-stream tidal turbine system. Part D Conference Proceeding of World Maritime Technology Conference (WMTC), 4th International Marine Renewable Energy, MAREC, London, 6–10 March 2006, pp. 89–95, IMarEST.

5 **Kelly, N. D., McKenna, H. E. R., Hemphill, R., Etter, C. L., Garrelts, R. C.,** and **Linn, N. C.** *Acoustic noise associated with the MOD-I wind turbine: its source, impact and control.* SERI TR-635-1166, National Renewable Energy Laboratory, Golden, Colorado, 1985.

6 **Glegg, S. A. L., Baxter, S. M.,** and **Glendinning, A. G.** The prediction of broadband noise for wind turbine. *J. Sound Vib.*, 1987, **118**(2), 217–239.

7 **Greene, G. C.** and **Hubbard, H. H.** *Some effect of non-uniform inflow on the radiated noise of a large wind turbine.* TM-8183, NASA Langley Research Center, Hampton, Virginia, 1980.

8 **Kelly, N. D., Hemphill, R. R.,** and **Sengupta, D. L.** Television interface and acoustic emission associated with the operation of the Darrieus VAWT. Proceedings of 5th Biennial Wind Energy Conference and Workshop, Washington, DC, 1981, vol. 1, pp. 397–413.

9 **Stephens, D. G., Shepherd, K. P., Hubbard, H. H.,** and **Grosveld, F. W.** *Guide to evaluation of human exposure to noise from large wind turbine.* M-83288, NASA Langley Research Center, Hampton, Virginia, 1982.

10 **Barnaby, S. W.** On the formation of cavities in water by screw propeller at high speed. *Transactions of the Institution of Naval Architects*, 1897, **38**, 139–144.

11 **Parsons, C.** The application of the compound steam turbine to the purpose of marine propulsion. *Transactions of the Institution of Naval Architects*, 1897, **38**, 232–242.

12 **Batten, W. M. J., Bahaj, A. S., Molland, A. F.,** and **Chaplin, J. R.** Hydrodynamics of marine current turbines. *Renew. Energy*, 2006, **31**(2), 249–256.

13 **Molland, A. F., Bahaj, A. S., Chaplin, J. R.,** and **Batten, W. M. J.** Measurements and predictions of forces, pressures and cavitation on 2-D sections suitable for marine current turbines. *Proc. Instn Mech. Engrs, Part M: J. Engineering for the Maritime Environment*, 2004, **218**, 127–138.

14 **Wang, D., Atlar, M.,** and **Mesbahi, E.** Experimental investigation of propeller wash using laser doppler anemometry. HIPER'02, 3rd International Conference on *High-performance marine vehicles*, Bergen, Norway, 14–17 September 2002.

15 **Wang, D., Atlar, M., Paterson, I., Danisman, D. B.,** and **Mesbahi, E.** *Slipstream (wash) measurements with model propeller of a catamaran in isolation using an LDA system.* FLOWMART, Report no MT-2001-008, Newcastle University, 2001.

16 **Wang, D., Atlar, M., Glover, E. J.,** and **Paterson, I.** Experimental investigation of flow field around a podded propulsor using LDA. T-POD, First International Conference on *Technological advances in podded propulsion*, Newcastle University, 14–16 April 2004, pp. 483–498.

17 **Atlar, M. A.** History of the emerson cavitation tunnel and its role in propeller cavitation research. NCT'50, International Conference on *Propeller cavitation*, Newcastle-upon-Tyne, April 2000, pp. 3–34.

18 **Somers, D. M.** *Design and experimental results for the S814 airfoil: Airfoil, Incorporated.* Subcontractor report: NREL/SR-440-6019, State College, Pennsylvania, 1997.

19 **ITTC.** Cavitation committee report. 15th International Towing Tank Conference, The Hague, the Netherlands, 1978.

20 **Ross, D.** *Mechanics of underwater noise*, 1976 (Pergamon Press, New York, USA).

21 **ITTC.** Cavitation committee report. 18th International Towing Tank Conference, Kobe, Japan, 1987.

22 **Mitson, R. B.**(Ed.) *Underwater noise of research vessels, review and recommendations.* Cooperative research report No 209, International Council For the Exploration of the Sea, May 1995.

APPENDIX

Notation

$C_{0.7R}$	chord length at 0.7 R (m)
$Cp_{\max}$	maximum power coefficient
D	diameter of the propeller (m)
f	centre frequency (Hz)
F_n	Froude number
g	acceleration of gravity (m/s^2)
Hs	shaft immersion of the turbine (m)
J	advance ratio
n	rotation rate of turbine shaft (1/s)
P	pressure at a point of interest (N/m^2)
p_a	pressure at atmosphere (N/m^2)
P_v	vapour pressure of water (N/m^2)
r	vertical reference distance for which the noise level is measured
r_h	hub radius (m)
R	radius of turbine (m)
R_e	Reynolds number
SPL	equivalent 1 Hz at 1 m distance sound pressure level (in dB; re 1 μPa)
SPL_B	background sound pressure level measured at an equivalent 1 Hz bandwidth and 1 m (in dB; re 1 μPa)
SPL_1	reduced sound pressure level to 1 Hz bandwidth (in dB; re 1 μPa)
SPL_m	measured sound pressure level at each centre frequency (in dB; re 1 μPa)
SPL_N	net sound pressure level calculated at equivalent 1 Hz bandwidth and 1 m (in dB; re 1 μPa).
SPL_T	total sound pressure level measured at an equivalent 1 Hz bandwidth and 1 m (in dB; re 1 μPa)
V_c	tidal stream speed or propeller inflow velocity (m/s)
V_R	resultant velocity of blade section (m/s)
V_{x_m}	mean axial velocity on a quadrant (m/s)
V_{z_m}	mean vertical velocity on a quadrant (m/s)
V_{x_pm}	mean axial velocity at a point (m/s)
V_{z_pm}	mean vertical velocity at a point (m/s)
V_{x_rm}	mean axial velocity on a radius (m/s)
V_{z_rm}	mean vertical velocity on a radius (m/s)
V_{x_t}	measured axial velocity in time domain represented by angle (m/s)

V_{z_t}	measured vertical velocity in time domain represented by angle (m/s)
V_{x_tm}	mean axial velocity at 5° interval in time domain (m/s)
V_{z_tm}	mean vertical velocity 5° interval in time domain (m/s)
α	gas content at the pressure at a point of interest
α_{s}	gas content at the atmospheric pressure
Δf	bandwidth for each one-third Octave band filter in Hz.
$\Delta L_{(P)}$	increased noise level when scaled from the model to full scale(in dB; re 1 μPa)
λ	tip speed ratio
ν	kinematic viscosity of water (m^2/s)
ρ	mass density of water (kg/m^3)
σ	cavitation number